JOURNAL OF GEOPHYSICAL RESEARCH, VOL. 102, NO. D25, PAGES 30,119–30,133, DECEMBER 27, 1997

Physical properties of Amazonian soils: A modeling study using the Anglo-Brazilian Amazonian Climate Observation Study data

C. Delire, J.-C. Calvet, and J. Noilhan

Météo-France/Centre National de la Recherche Météorologique, Toulouse, France

I. Wright

Institute of Hydrology, Wallingford, England, United Kingdom

A. Manzi and C. Nobre

Centro de Previsão de Tempo e Estudios Climaticos, Instituto Nacional de Pesquisas Espaciais Cachoeira-Paulista, Brazil

Abstract. The hydraulic properties of some Amazonian soils differ significantly from the properties of the temperate soils. Most of the soil water release functions implemented in the atmospheric models used in deforestation studies were developed for temperate soils. It is necessary to check the validity of these soil water models with in situ data. In this study, the Anglo-Brazilian Amazonian Climate Observation Study (ABRACOS) soil data have been used to modify the parameter values of Clapp and Hornberger's water release model. Different relations between hydraulic parameters and texture are proposed. These relations are included in the ISBA land surface scheme which is used to simulate the long-term evolution of the soil water content and the surface energy balance of three contrasting ABRACOS sites: two pasture sites with distinct soil properties and a forest site. The sensitivity of the simulations to the use of either the original Clapp and Hornberger water release model or the ABRACOS-derived one is shown.

1. Introduction

The deforestation of the Amazonian basin occurs at a rate and a scale which might have an important impact on the regional and global climate. Several numerical experiments have been performed with general circulation models in order to quantify this impact [e.g., *Dickinson and Henderson-Sellers*, 1988; *Lean and Warrilow*, 1989; *Nobre et al.*, 1991; *Eltahir and Bras*, 1993; *Polcher and Laval*, 1994; *Manzi and Planton*, 1996; *Zhang et al.*, 1996]. Results of these experiments agree in predicting higher surface temperature but disagree in evaluating the impact on the hydrological cycle. In particular, it is not clear whether deforestation leads to increased or decreased precipitation. These numerical experiments are mainly sensitivity studies to the modification of the surface parameters. The quality of the results is therefore highly dependent on the realism of the representation of the soil-vegetation-atmosphere interactions. In order to improve, calibrate and validate land surface parameterization schemes, it is necessary to obtain realistic surface parameters and meteorological data for both the forested and deforested areas. The physical properties of the Amazonian rain forest were studied during the Amazon Region Micrometeorological Experiment (ARME) and have been described by *Shuttleworth et al.* [1984] and *Shuttleworth* [1988]. This data set has been used to calibrate land surface schemes [*Sellers et al.*, 1986]. More recently, the Anglo-Brazilian Amazonian Climate Observation Study (ABRACOS) provided information on the surface-atmosphere interactions in both forested and deforested areas at different locations in the Amazon basin. Some of these data were used to calibrate the simplified simple biosphere model (SSiB) [*Xue et al.*, 1996], the second version of the simple biosphere model (SiB2) [*da Rocha et al.*, 1996a] and the one-dimensional single column atmospheric model (SiB-1D) [*da Rocha et al.*, 1996b].

This experiment also documented the physical properties of representative Amazonian soils [*Wright et al.*, 1996]. It revealed that the characteristics of some widespread Amazonian soils differ very significantly from what is observed in temperate regions. At a site near Manaus, for instance, the mean clay content exceeds 75% but the soil is rapidly drained like a sandy soil in temperate regions. This type of soil does not fit in the often used *Clapp and Hornberger* [1978] textural classes, for which the maximum clay content is only about 65%. Moreover, in the currently used soil water models which were derived from statistical analysis of temperate soil samples (see *Kern* [1995] for a review), the hydraulic conductivity decreases with higher clay contents. The use of these soil water models and classical textural classifications in land surface schemes may lead to important errors in the prediction of the available water content under forested and deforested areas of Amazonia. Unrealistic prediction of the water content can alter the simulation of the surface energy balance and affect the boundary layer development [*Cuenca et al.*, 1996].

In this paper, the land surface scheme ISBA [*Noilhan and Planton*, 1989] is tested against ABRACOS data. The ISBA scheme uses the *Clapp and Hornberger* [1978] soil water model, which is common to a large number of surface parameterization schemes used in atmospheric modeling. Our purpose is to determine whether Clapp and Hornberger's parameters can be modified in order to take into account in a more accurate way the properties of the Amazonian soils. After a brief description

Paper number 97JD01836.
0148-0227/97/97JD-01836$09.00

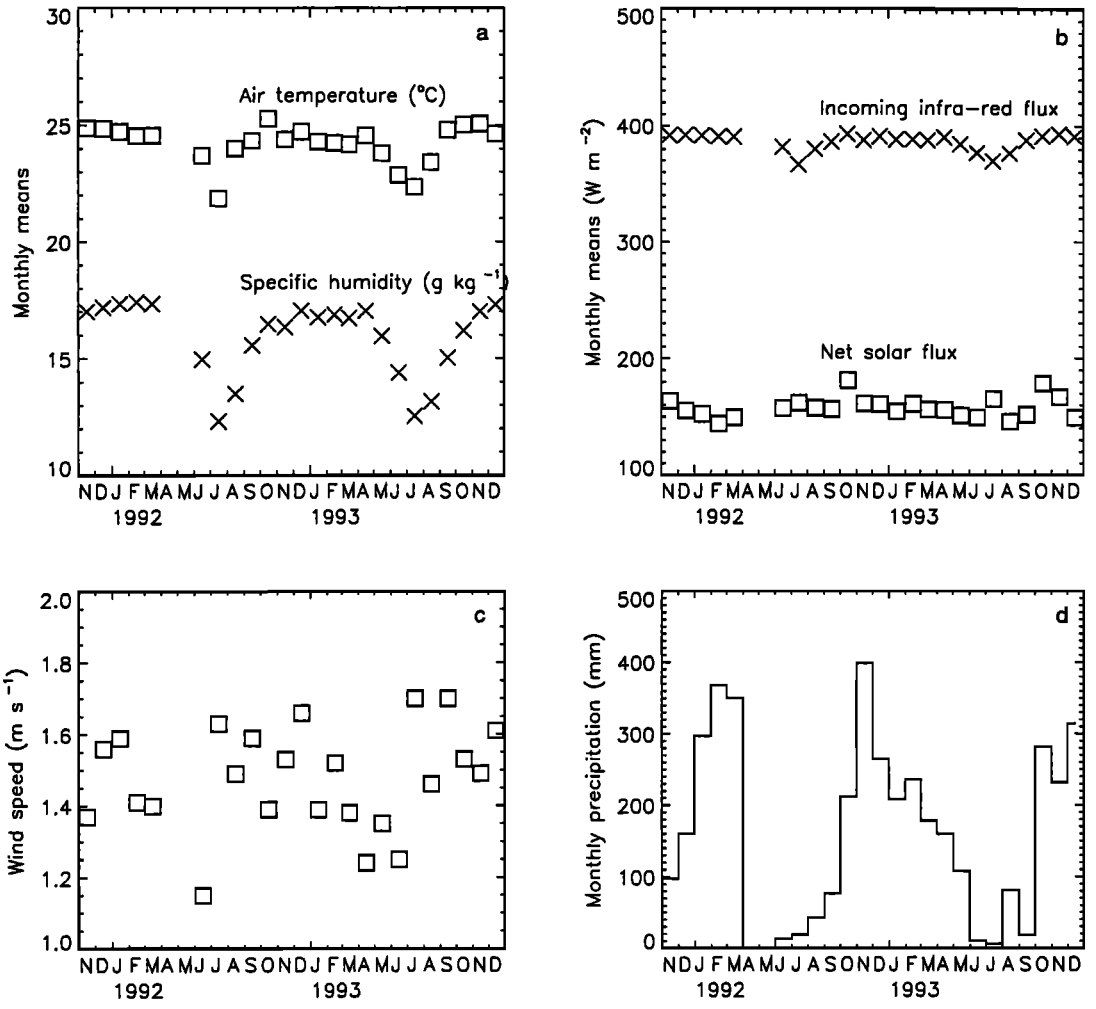

Figure 1. (a) Monthly means of observed reference level air temperature and specific humidity. (b) Monthly means of evaluated incoming infrared and observed net shortwave flux. (c) Monthly means of observed wind speed. (d) Monthly precipitation.

of the ABRACOS field experiment, the characteristics of the Amazonian soils are investigated. The measured vertical profiles of soil texture, critical water contents and soil hydraulic parameters at five ABRACOS sites are used to derive, when possible, modified relationships between texture and Clapp and Hornberger's parameters and the soil-related parameters of ISBA. Measured surface fluxes during short periods of the ABRACOS experiment are then used to calibrate two vegetation parameters of ISBA in section 4. Section 5 presents long-term simulations of the water content at three ABRACOS sites and a sensitivity study to the modified description of the soil physical properties in ISBA.

2. The ABRACOS Field Experiment

The Anglo-Brazilian Amazonian Climate Observation Study was designed to obtain comparative micrometeorological, climatological, hydrological, and physiological data from adjacent forested and deforested sites in Brazilian Amazonia [*Gash et al.*, 1996]. It started at the end of 1990 and lasted 4 years. From the six principal ABRACOS sites described by *Gash et al.* [1996], three sites have been chosen for this study: one forest site and two pasture sites with completely different soil properties. The forest site (Jaru Reserve Forest (JRF), 120 m, 10°05'S, 61°55'W) and one of the pasture sites (Nossa Senhora Pasture (NSP), 220 m, 10°45'S, 62°22'W) are located in the state of Rondônia where extensive deforestation has taken place in the last two decades. The second pasture site (Fazenda Dimona Pasture (FDP), 120 m, 2°19'S, 60°19'W) is located near Manaus in the state of Amazonas, a state with little forest clearance. At least 2 years of weekly soil moisture records and reference level atmospheric variables are available for these three sites. The surface fluxes were also measured during intensive field campaigns lasting several weeks. The soil thermal and hydraulic properties of these sites were discussed by *Wright et al.* [1996], who pointed out that these sites are close to the textural extremes of Amazonian soils.

Figure 1 shows the monthly means of precipitation, shortwave net radiation, and reference level air temperature, specific humidity, and wind measured by the automatic weather stations at NSP between November 1991 and December 1993. Months with more than 20% missing data are skipped (April and May 1992). The long-wave radiation, which was not measured, is estimated using the *Staley and Jurica* [1972] parameterization. The meteorological conditions at the nearby JRF

Table 1. Surface and Soil Parameters

Site	NSP	JRF	FDP
Vegetation type	grass	forest	grass
Root depth (d_2), m	2	≥4	1.5
Vegetation cover (veg)	0.85	0.99	0.85
Vegetation height, m	0.6	30	0.3
Roughness length for momentum (Z_0), m	0.1h	2.6	0.1h
Leaf area index (LAI)	1.5–3.9	4.6	1.5
Albedo	0.180–0.210	0.120–0.144	0.155–0.190
Canopy storage capacity ($W_{r\max}$), mm	...	1.03	...
Mean clay content, %	30	24	76
Mean sand content, %	60	63	12
Height of the temperature measurement, m	5.1	52.5	1.2
Height of the wind measurements, m	5.4	52.5	2.
Displacement height, m	0.4	25.8	0.18

Values are from *Wright et al.* [1996].

forest site are not very different. Both sites are located near the southwestern border of the Amazonian basin and experience a marked seasonal cycle in the rainfall regime. The dry season extends from June to August, while the wettest period goes from November to March. The dry season also coincides with colder and dryer air. The FDP site near Manaus has wetter conditions all year round with still substantial rainfall during the dry period between June and August.

2.1. Nossa Senhora Pasture (NSP), Ji-Paraná, Rondônia

This cattle ranch site was deforested 15 years ago [*Culf et al.*, 1995] and is located in an area where deforestation occurred following a characteristic fishbone pattern which can be observed on high-resolution satellite images [*Gash et al.*, 1996; *Calvet et al.*, 1997]. In this region, grasslands are separated by strips of forest of variable size depending on the extent of the deforestation. The vegetation, a drought-tolerant grass, is described in detail by *McWilliam et al.* [1996], and some characteristic parameters are summarized in Table 1. The effective rooting depth given in Table 1 was defined by *Wright et al.* [1996] as the depth at which 95% of soil moisture changes occur over a 2 year period. During the dry season the leaf area index (LAI) is minimal while the albedo is maximum. Monthly values of these two parameters are given by *McWilliam et al.* [1996] and *Culf et al.* [1995]. Near the surface the soil is mainly sandy (85% of sand) [*Hodnett et al.*, 1996a]. The clay content increases gradually with depth from 7% near the surface to 35% at 1 m.

2.2. Jaru Reserve Forest (JRF), Ji-Paraná, Rondônia

This forest site is established in an ecological reserve, 90 km northwest of Fazenda Nossa Senhora. During ABRACOS, there was no clearance within a region of 30 km radius. It is a primary open tropical forest [*RADAMBRASIL Projeto*, 1978] with a mean canopy height of 30 m. Roots have been found as deep as 3.5 m (Table 1), but it seems that the trees are able to extract water from below since it was not possible to detect any significant decrease in forest transpiration during the dry season when the moisture content within the 3.6 m of the soil surface was low [*Wright et al.*, 1996]. The soil texture is similar to that of NSP.

2.3. Fazenda Dimona Pasture (FDP), Manaus, Amazonas

Fazenda Dimona is a 10 km^2 cattle ranch, located about 100 km north of Manaus, in a region with little forest clearance [*Gash et al.*, 1996]. The site was burned several times until the end of 1992 to prevent shrub regrowth. Shrub cover increased from 2% at the end of 1992 to 30% in July 1993 [*Hodnett et al.*, 1996a]. The leaf area index was only measured during the dry season, and the value reported in Table 1 can be taken to be a minimum value [*Roberts et al.*, 1996]. Soil at FDP has been the subject of numerous studies [*Wright et al.*, 1992; *Hodnett et al.*, 1995, 1996a]. The link between textural and hydraulic properties of this soil has no analogue in temperate regions. This soil has a very high clay content, from 65% near the surface to 80% at a depth of 0.75 m, with porosity between 55% and 60%. Despite the high clay content this soil is drained very rapidly because of the presence of macropores [*Hodnett et al.*, 1996a] which are the result of the intense biological activity under the original forest [*Tomasella and Hodnett*, 1996]. Consequently, the available water capacity for plants is rather low, about 70 mm in the upper meter. Data from this site have already been used to calibrate the SSiB [*Xue et al.*, 1996] and the SiB2 models [*da Rocha et al.*, 1996a].

3. Description of Amazonian Soil Properties for Surface Modeling

In the original ISBA model (briefly described in the appendix), the transfer coefficients for heat and moisture (C_g, C_1, C_2, C_3) and the critical volumetric water contents ($w_{\rm sat}$, w_{fc}, $w_{\rm wilt}$) were determined using the statistical description of soil hydraulic and thermal properties proposed by *Clapp and Hornberger* [1978] and *McCumber and Pielke* [1981]. In these parameterizations, the saturated hydraulic conductivity $K_{\rm sat}$, the saturated water content $w_{\rm sat}$ and the slope of the retention curve b, are related to the soil texture and are evaluated for 11 textural classes. This study was based on a statistical analysis of 1000 U.S. soil samples. From these 11 textural classes, *Noilhan and Lacarrère* [1995] derived, for aggregation purposes, continuous relationships between clay or sand content and the critical water contents ($w_{\rm sat}$, w_{fc}, $w_{\rm wilt}$), the slope of the retention curve b, and the reference value of the transfer coefficients ($C_{g\rm sat}$, $C_{1\rm sat}$, $C_{2\rm ref}$, C_3) (see Table 2). As pointed out by *Tomasella and Hodnett* [1996], the moisture retention properties of Amazonian soils are not typical of temperate soils. It is therefore necessary to check the validity of the soil transfer coefficients and critical water contents deduced from Clapp and Hornberger's model.

Measured and optimized vertical profiles of saturated water content, residual water content, saturated hydraulic conductivity, dry bulk density, and clay and sand content are summarized

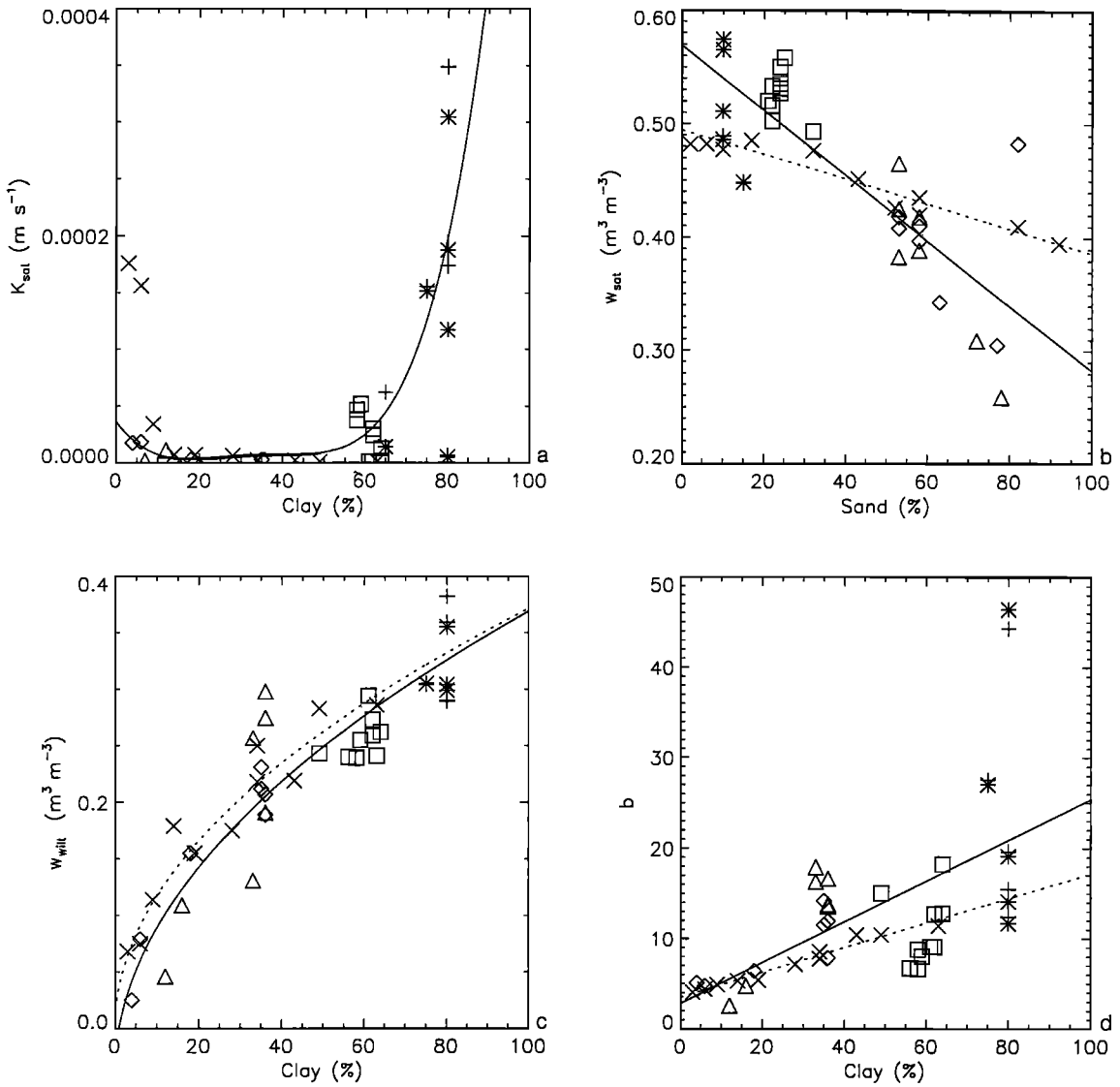

Figure 2. Plots of measured hydraulic parameters (a) K_{sat}, (b) w_{sat}, and (c) w_{wilt} and calculated hydraulic parameters (d) b, (e) w_{fc}, (f) C_{2ref}, and (g) C_3 at different depths at the five ABRACOS sites versus clay or sand content or versus saturation hydraulic conductivity K_{sat}. The solid line corresponds to the new regression curve (ISBA-NEW, Table 3). The dotted line corresponds to the original ISBA curve (ISBA-OLD, Table 2). Values of the parameters for the Clapp and Hornberger textural classes are also plotted but were not used for the regression analysis.

in Table 2 of *Wright et al.* [1996] for five ABRACOS sites. The fitting parameters of the van Genuchten water release model [*van Genuchten*, 1980] are also given in Table 2 of *Wright et al.* [1996]. There is considerable use of the van Genuchten functions in the soil physics community, while there is almost no current use of the Clapp and Hornberger functions. The opposite relation exists for the atmospheric modeling community, which uses the Clapp and Hornberger relations which were first applied in mesoscale models.

In this study the data summarized in Table 2 of *Wright et al.* [1996] are used to modify the original continuous relations [*Noilhan and Lacarrère*, 1995] between the soil texture and the hydraulic and thermal parameters of ISBA (K_{sat}, b, C_{gsat}, C_{1sat}, C_{2ref}, C_{3ref}, w_{sat}, w_{fc}, w_{wilt}) for the Amazonian soils.

Table 2. Relations Between Hydric and Thermal Parameters in the Original Version of ISBA (ISBA-OLD)

Parameter	Formula
b	3.501 + 0.137(clay)
w_{sat}	0.494 − 0.001(sand)
w_{fc}	$0.08905(\text{clay})^{0.3496}$
w_{wilt}	$0.03713(\text{clay})^{1/2}$
C_{gsat}	−0.01557(sand) − 0.01441(clay) + 4.7021
C_{1sat}	$0.8488 + 0.00558(\text{clay})^{1/2}$
C_{2ref}	$13.815(\text{clay})^{-0.954}$
C_3	$5.327(\text{clay})^{-1.043}$

Formulas are from *Noilhan and Lacarrère* [1995]. The sand and clay contents (i.e., sand and clay) are expressed in percentage.

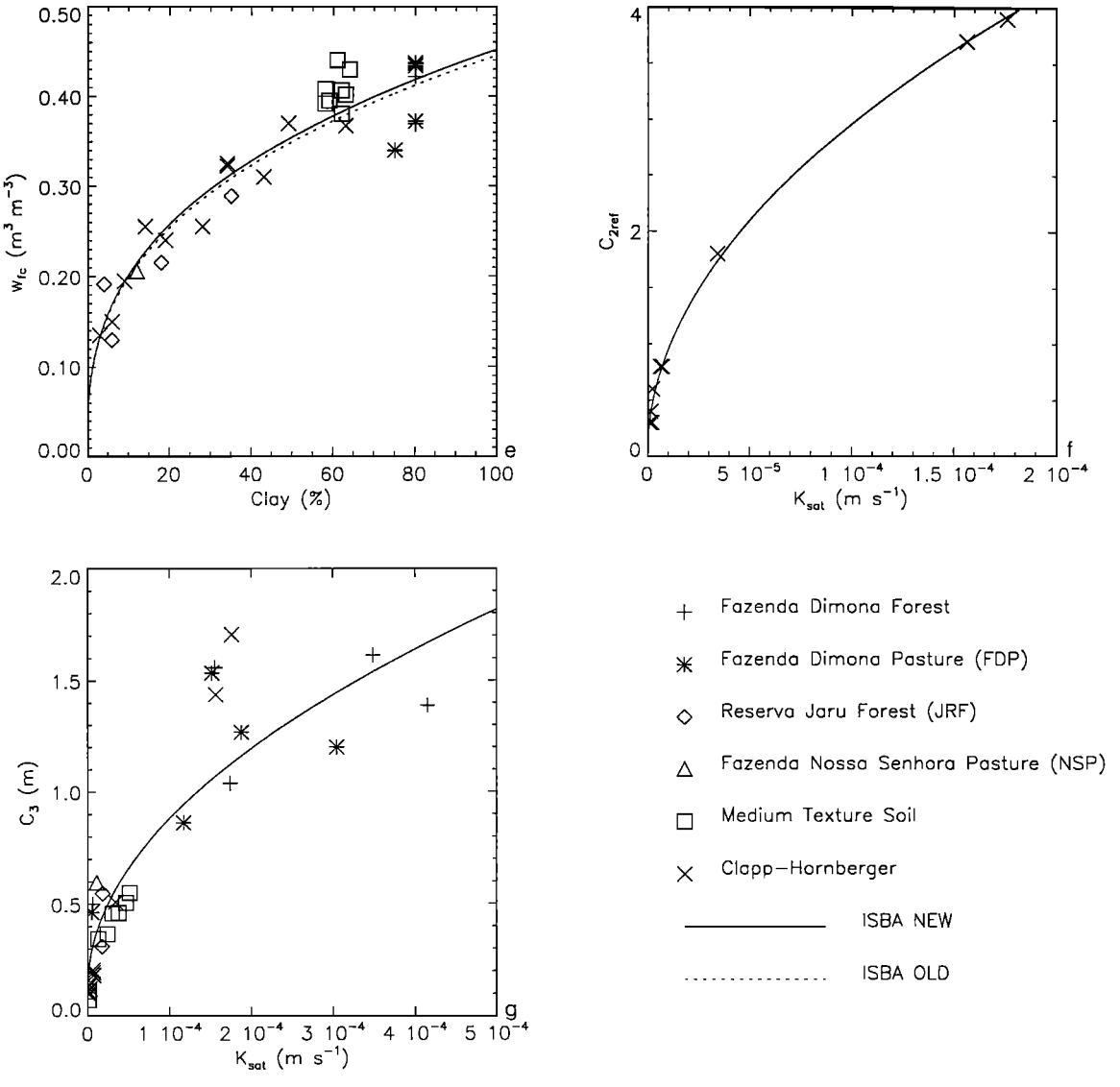

Figure 2. (continued)

The values of the considered parameters corresponding to the different depths and locations are used as independent data in order to perform linear regressions and power law adjustments for each parameter as a function of clay or sand content. The order of the polynomial is kept identical to the one chosen by *Noilhan and Lacarrère* [1995]. Continuous relations between texture and hydraulic properties are useful when coupling the land surface scheme with a mesoscale atmospheric model. The textural information is not always available at the horizontal resolution of the mesoscale model, and a regridding procedure is necessary. Simple averages are possible with percentages of sand or clay, but not with textural types, for instance.

The most striking difference between the Amazonian soils studied here and the temperate soils used for Clapp and Hornberger's analysis is the saturated hydraulic conductivity, K_{sat}. Figure 2a shows measured and optimized values of K_{sat} for the five Amazonian sites treated by *Wright et al.* [1996] together with the Clapp and Hornberger values for the 11 textural classes. It appears that for the Amazonian soils, K_{sat} is high for clayey soils and low for sandy soils whereas the reverse behavior is usually observed for temperate soils. The highest values of K_{sat} are found at FDP and at the nearby forest site. As mentioned before, unlike other clay soils, K_{sat} is very high, reaching values more characteristic of a sandy soil in temperate regions. This behavior can be explained by the presence of macropores between 0.4 and 1.1 m resulting from the activity of ants, termites, and worms under the original forest [*Tomasella and Hodnett*, 1996]. On the other hand, the hydraulic conductivity of the sandy soil of JRF and NSP is rather low in comparison with the conductivity of the equivalent Clapp-Hornberger textural class. In the case of the pasture site, this small conductivity in the first 20 cm is probably due to soil compaction by cattle [*Wright et al.*, 1996]. Figure 2a presents K_{sat} as a function of the clay content. In spite of the important dispersion of the conductivity data, a fourth-order polynomial was fitted to the Amazonian data with a square regression coefficient (r^2) of 50% (Table 3).

The saturation water content w_{sat} evolves in a more usual way with a clear correspondence between high saturation volumetric moisture contents and low percentages of sand (Figure 2b). However, the maximum values observed in the case of FDP are much higher than those given in the Clapp and Horn-

Table 3. Relations Between Hydric and Thermal Parameters Deduced From the ABRACOS Data

Parameter	Formula
K_{sat}	$3.66 \times 10^{-5} - 5.04 \times 10^{-6}$ clay $+ 2.69 \times 10^{-7}$ clay^2 $- 5.62 \times 10^{-9}$ clay^3 $+ 4.28 \times 10^{-11}$ clay^4
b	2.8 + 0.226(clay)
w_{sat}	0.569 − 0.003(sand)
w_{fc}	$0.0903(\text{clay})^{0.3496}$
w_{wilt}	$-0.0404 + 0.0409(\text{clay})^{1/2}$ if clay $\geq 1\%$
C_{1sat}	[5.58(clay) + 84.88](1000.) if clay $\leq 63\%$
	4.36×10^5 if clay $\geq 63\%$
C_{2ref}	$0.012 + 0.3[K_{sat}(10^6)]^{1/2}$
C_3	$0.107 + 0.073[K_{sat}(10^6)]^{1/2}$

Formulas are from *Wright et al.* [1996]. The sand and clay contents (i.e., sand and clay) are expressed in percentage.

berger data set. This might be explained by the higher clay concentration and the macroporosity. A linear relation was fitted with $r^2 = 67\%$ indicative of the rather important dispersion of the data. The wilting point values (Figure 2c), taken as the measured residual moisture contents, are less dispersed ($r^2 = 80\%$) and similar to the original ISBA values.

The other parameters of ISBA cannot be directly deduced from the available measured data. The slope of the retention curve in Clapp and Hornberger's model, b, was derived comparing the van Genuchten water release model [*van Genuchten*, 1980] with the fitting parameters values given by *Tomasella and Hodnett* [1996] or *Wright et al.* [1996] and the Clapp and Hornberger model. This procedure was necessary because only the van Genuchten fitting parameters were available. Following *van Genuchten* [1980] and *Mualem* [1976], the hydraulic conductivity is given as

$$K(S_w) = K_{sat} S_w^l [1 - (1 - S_w^{n/(n-1)})^{(n-1)/n}]^2 \quad (1)$$

where l and n are dimensionless fitting parameters, and S_w is the effective saturation fraction given as

$$S_w = \frac{w - w_r}{w_{sat} - w_r} \quad (2)$$

with w_r the residual volumetric water content taken here as the wilting point. Equating (1) with the equivalent Clapp and Hornberger relation for the hydraulic conductivity,

$$K(w) = K_{sat}(w/w_{sat})^{2b+3} \quad (3)$$

gives

$$b = \frac{1}{2}\left[\frac{\ln (S_w^l[1 - (1 - S_w^{n/(n-1)})^{(n-1)/n}]^2)}{\ln (w/w_{sat})} - 3\right] \quad (4)$$

In the original Clapp and Hornberger model, the b parameter depends only on soil texture. In (4), b still depends on the volumetric water content. However, the variation is quite slow (less than 10%) for effective saturation fractions between 0.3 and 0.7. We used the value $S_w = 0.5$ with the values of l and n given in Table 2 of *Wright et al.* [1996] in (4) to determine the b parameter presented in Figure 2d. The wide range of values of K_{sat} (Figure 2a) observed under the pasture and forest sites of Fazenda Dimona is mostly responsible for the scattered calculated b ($r^2 = 31\%$). Maximum values of b (more than 40) are much higher than those of Clapp and Hornberger. These high values of b are found at the Fazenda Dimona sites and are also a consequence of the macroporosity. For low water content, the hydraulic conductivity has values similar to the hydraulic conductivity of clay soils in temperate regions [*Tomasella and Hodnett*, 1996]. For high water content, macropores enhance the percolation process. This is reflected by the high values of b, implying a sharp increase of the hydraulic conductivity with the water content.

The field capacity in ISBA was selected as that water content associated with a hydraulic conductivity of 0.1 mm/d [*Jacquemin and Noilhan*, 1990]. It is obtained by inverting equation (3):

$$w_{fc} = w_{sat}(K_{fc}/K_{sat})^{1/(2b+3)} \quad (5)$$

where K_{fc} is the hydraulic conductivity at field capacity, taken as 0.1 mm/d. In contrast with the other critical water contents of the ABRACOS soils, the relation between field capacities and texture is very similar to that of ISBA for normal temperate soils (Figure 2e).

The coefficient C_2 (equation (A9)) characterizes the rate at which the water profile is restored to equilibrium between gravity and retention [*Noilhan and Planton*, 1989]. Its reference value C_{2ref} is linked to the hydraulic conductivity and was directly related to the clay content in the original ISBA scheme [*Noilhan and Lacarrère*, 1995]. Because of the reverse behavior of K_{sat} with clay content in this data set, we preferred to use directly the functional link between C_{2ref} and K_{sat} deduced from the 11 Clapp and Hornberger textural classes as shown in Figure 2f.

The rate at which the water profile is restored to the field capacity by gravitational drainage is specified by the C_3 coefficient [*Mahfouf and Noilhan*, 1996], which is also linked to the hydraulic conductivity. Instead of using the textural dependency proposed by *Mahfouf and Noilhan* [1996], C_3 was estimated with its analytical expression given in the appendix (equation (A10)). Figure 2g shows the calculated C_3 versus the saturated hydraulic conductivity for the ABRACOS data set and the 11 Clapp and Hornberger textural classes. In this case the Amazonian values differ noticeably from the original ISBA ones.

The saturation value of the hydraulic transfer coefficient C_{1sat} (equation (A8)) depends on w_{sat}, K_{sat}, b, and ψ_{sat}, the matric potential at saturation [*Noilhan and Planton*, 1989]. The latter is not directly available, because van Genuchten assumes zero saturation matric potential in its power curve representing the moisture characteristic. However, ψ_{sat} can be approximated by the matric potential near saturation as suggested by Clapp and Hornberger. The ψ_{sat} obtained in this way gives a very scattered diagram of C_{1sat} versus K_{sat} or clay content (not shown). This is why the *Noilhan and Lacarrère* [1995] formulation of C_{1sat} was adopted with a maximum threshold corresponding to the maximum Clapp and Hornberger clay content (Table 3).

The thermal transfer coefficient for bare soil C_g depends on the thermal diffusivity κ ($m^2\ s^{-1}$) and the volumetric heat capacity C ($J\ m^{-3}\ K^{-1}$) of soils [*Bhumralkar*, 1975], which are both linked to the moisture content. It was approximated with a power law by *Noilhan and Planton* [1989] (equation (A7)). In order to check the validity of this power law for the Amazonian soils, C_g was calculated using published values of the thermal diffusivity κ and the volumetric heat capacity C [*Alvalá et al.*, 1996]. Despite the lack of data, the power law seems to work well for the FDP site but overestimates C_g at NSP, at least for the very small water contents that are observed near the soil surface (Figure 3). However, the original ISBA power law was

kept. This is because, first, there are not enough data to derive another parameterization and also because the total volumetric soil moisture content in the root zone (2 m) observed at NSP is always much higher than the very small values observed near the soil surface (see section 5).

A comment should be made on the validity of Clapp and Hornberger and the van Genuchten water release models. The fundamental reason the Clapp and Hornberger functions do not fit Amazonian soils, which would be the same for the van Genuchten functions, is because basing soil hydraulic properties only on soil texture is not sufficient. This is the reason for the increased interest in the soil physics community for pedotransfer functions which start with soil texture and add additional properties such as particle size distribution to the parameter-fitting scheme. However, those data are not yet available in the ABRACOS case. Another possibility would be to include the kind of relation used by *Stieglitz et al.* [1997] for the saturated hydraulic conductivity which varies with depth and depends not only on the soil texture but also on the vegetation cover.

4. Model Calibration

Most of the ISBA parameters are already fixed by measurements (see Table 1). The only tunable parameters are the minimum stomatal resistance $R_{s\min}$, the vegetation heat transfer coefficient C_v, and the ratio between roughness lengths for momentum and heat (Z_0/Z_{0h}). This ratio was fixed to a value of 10 already used by *Manzi and Planton* [1996] in a simulation for the FDP site. The calibration has been done with the adapted version of ISBA ("NEW") taking into account the hydrological properties of the Amazonian soils described before. The flux measurements used to calibrate ISBA were collected during the intensive field campaigns described by *Gash et al.* [1996]. These data consist of hourly estimates of net radiation R_n, soil heat flux G, sensible heat flux H, and latent heat flux LE. The soil heat flux G is used to calibrate C_v, and $R_{s\min}$ is determined by the four fluxes. The calibration was

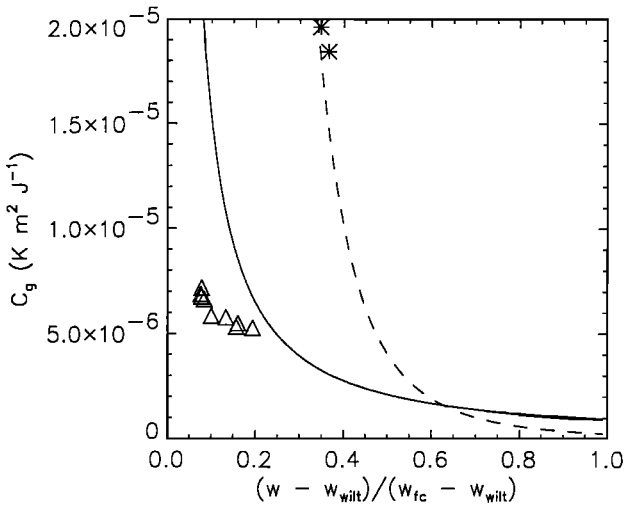

Figure 3. Calculated values of the bare soil heat transfer coefficient C_g using observed values of the thermal diffusivity for the Fazenda Dimona (asterisks) and Nossa Senhora (triangles) pasture sites versus soil moisture content. The solid (dashed) lines represents the approximated power curve used in ISBA for the NSP (FDP) site.

Table 4. Optimized Values of the Heat Transfer Coefficient for Vegetation C_v and the Minimum Surface Resistance $R_{s\min}$

Site	NSP	JRF	FDP
C_v, K m^2 J^{-1}	5×10^{-3}	1.2×10^{-5}	0.4×10^{-3}
$R_{s\min}$, s m^{-1}	132	175	197
R_n, W m^{-2}			
rms error	27	29	20
Mean bias	−2	7	1
H, W m^{-2}			
rms error	43	28	19
Mean bias	3	9	3
LE, W m^{-2}			
rms error	53	37	23
Mean bias	−10	−1	−1
G, W m^{-2}			
rms error	24	26	15
Mean bias	6	1	−1

done separately on C_v and $R_{s\min}$. The optimization implies "off-line" runs of ISBA forced by measured values of air temperature, specific humidity, wind speed, net solar and longwave radiations, and precipitation. The quality of the simulation is assessed by a function measuring the deviation between calculated and observed variables. The optimization of C_v is performed before the optimization of $R_{s\min}$. In the case of C_v, the function measuring the quality of the simulation is the mean square error between hourly average simulated soil heat flux, and hourly observed soil heat flux. In the case of $R_{s\min}$, the function is the sum of the mean square errors on the four surface fluxes. The operation is repeated iteratively on C_v and $R_{s\min}$. Data from the various missions for a single site are treated consecutively as if they were part of the same data set. Except for JRF, where soil moisture measurements are limited to a depth of 3.6 m, the soil moisture content in the model is reinitialized to the observed value at the beginning of each mission. The time step used for each run is 300 s. For JRF the simulated soil heat flux was compared to the residual of the observed energy balance ($Rn_{\text{obs}} - H_{\text{obs}} - LE_{\text{obs}}$), which is not identical to the measured soil heat flux because of the important heat storage in the canopy [*Moore and Fisch*, 1986]. As mentioned before, ISBA considers only one energy balance for the whole ground-vegetation system. As a result, the simulated soil heat flux represents the total heat flux entering the vegetation, the canopy air, and the soil.

Optimized values of C_v and $R_{s\min}$ are given in Table 4 together with the root mean square error and the mean bias on the four fluxes. Significant negative values of the latent heat flux were observed at nighttime (about −50 W m^2) at NSP. The validity of these data is questionable since a positive sensible heat flux was measured at the same time. Therefore the optimization procedure for this site was used only with daytime values. Calculated versus observed values of the surface fluxes for this forest site are presented in Figure 4.

The sensitivity of the simulated fluxes on the calibrated parameters is illustrated in Figure 5. The sensitivity of the soil heat flux to the heat transfer coefficient C_v is similar for the two pasture sites. The error decreases rapidly for increasing values of C_v below 10^{-4} K m^2 J^{-1}. For higher values of C_v, the soil heat flux is more sensitive to changes of the bare soil transfer coefficient C_g than to the vegetation transfer coefficient C_v (equation (A6)). For the forest site (JRF) the error is minimal for C_v, around 10^{-5} K m^2 J^{-1}, and increases for

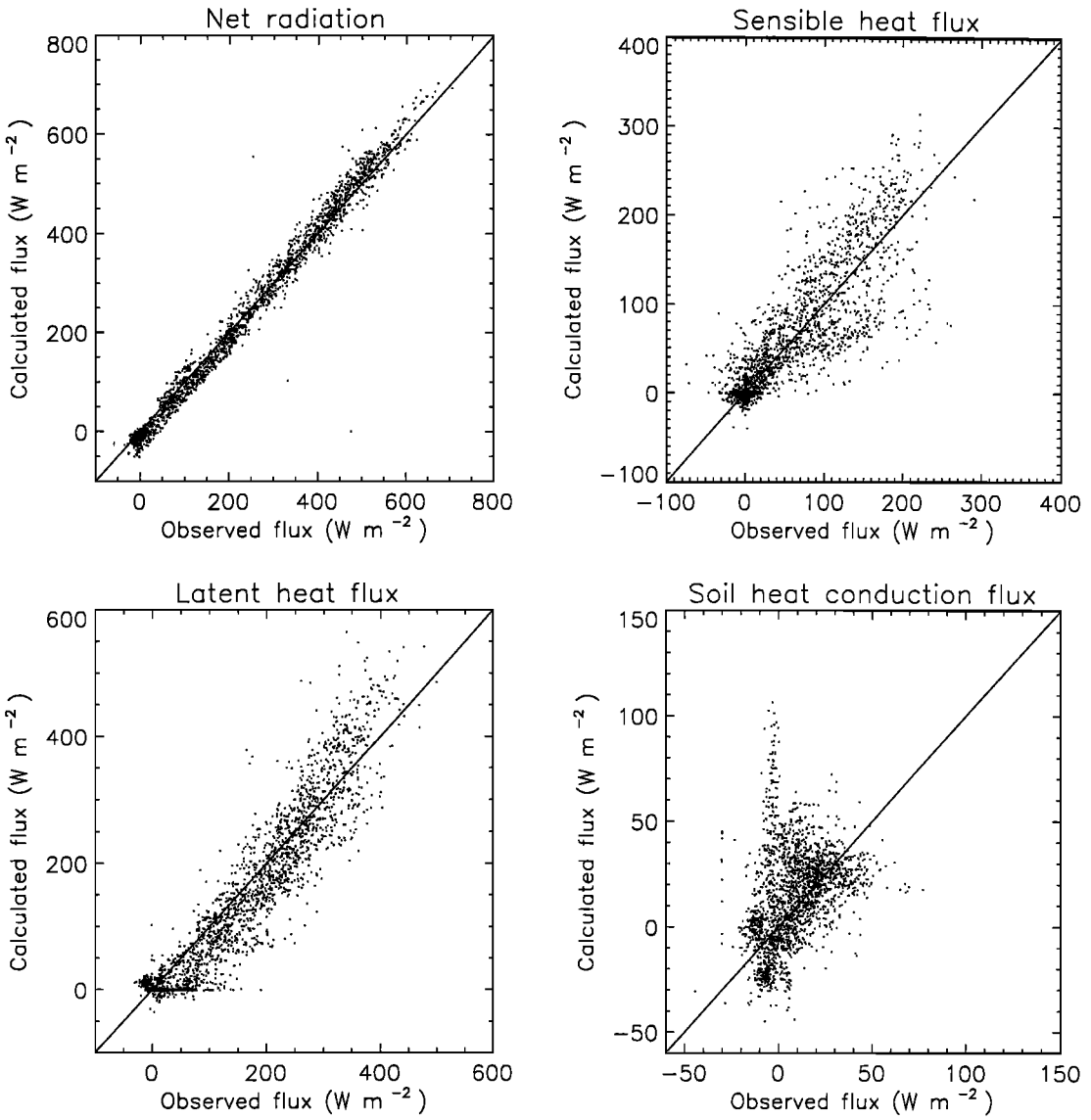

Figure 4. Calculated versus observed surface fluxes for daytime at Nossa Senhora pasture (NSP). Measurements were taken during three intensive field experiments.

higher values. In this case the fraction of bare soil (1%) is too small to influence the soil heat flux.

Figure 5b presents the sum of the root mean square errors between hourly averages of simulated and observed surface fluxes (R_n, LE, H, and G) versus $R_{s\min}$. Larger vegetation cover for forest as compared with pasture explains the higher sensitivity of the surface fluxes to the minimum surface resistance.

It should be noted that this optimization was realized with the available data lasting for short periods, mostly during the dry season. More measurements are needed to calibrate the model on a total seasonal cycle in order to simulate the long-term evolution of the surface fluxes.

5. Long-Term Simulation of the Water Content

Several annual cycles of soil moisture were simulated using the atmospheric and radiative forcing presented in section 2. As was done for the model calibration, the measured net solar radiation has been used as radiative forcing. The runs are performed with the adapted version of ISBA (ISBA-NEW) taking into account the physical properties of the Amazonian soils mentioned before. The soil and vegetation parameters used are those taken for the calibration of the model (Table 1) with the optimized values of C_v and $R_{s\min}$. Since some forcing data are missing, ISBA-NEW is run successively over the periods of continuous measurements. The observed soil moisture content at the beginning of each of these periods is taken as initial water content in the model. The resulting volumetric water content over the total rooting depth is compared with the available weekly neutron soundings. A full description and analysis of the soil moisture data set is given by *Hodnett et al.* [1996a, b]. Data at the pasture site of FDP are used to assess the sensitivity of simulated water budget and surface fluxes to the modified description of the soil physical properties in ISBA.

5.1. Nossa Senhora Pasture

Two years of simulation are performed at this pasture site with the modified version of ISBA (ISBA-NEW). Measured

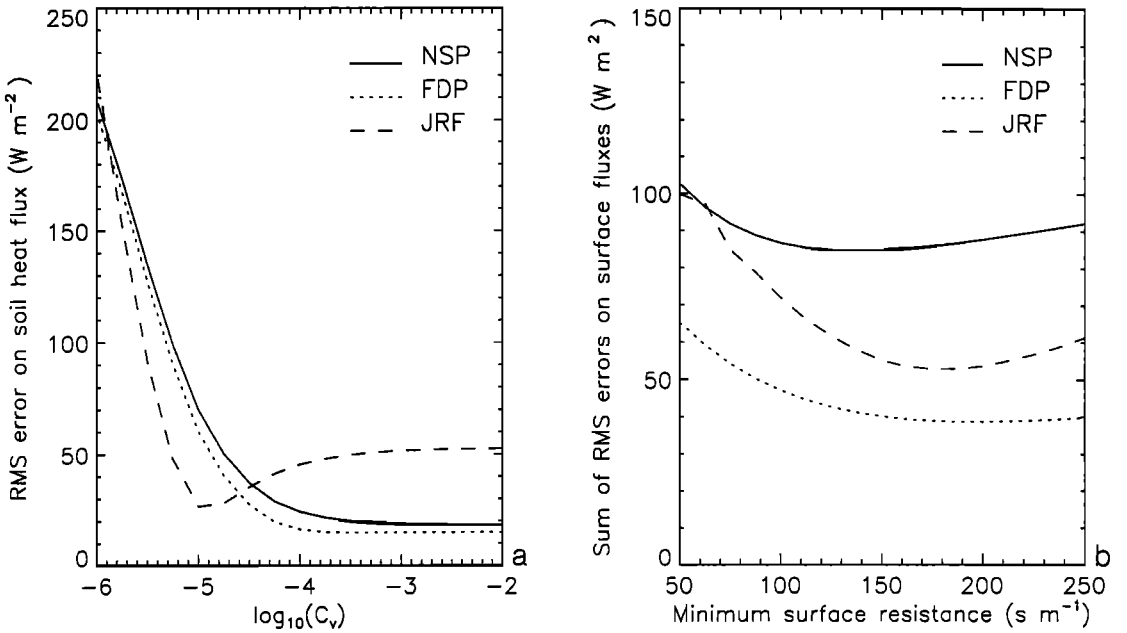

Figure 5. (a) Root mean square error between hourly averages of simulated and observed soil heat flux for different values of the vegetation heat transfer coefficient C_v. (b) Sum of the root mean square errors between hourly averages of simulated and observed surface fluxes (net radiation, latent heat, sensible heat, and soil heat fluxes) versus the minimum surface conductance.

values of the leaf area index [*Roberts et al.*, 1996] are taken when they are available (April, June, August, and September). A linear relation between the leaf area index and the monthly precipitation was used for the rest of the year. Figure 6 presents the evolution of the simulated and observed volumetric water content together with the measured rainfall. The simulated water content is very close to the observations, except from August to December 1992, when the simulated content is highly underestimated. The rather small amount of precipitation during this period leads us to believe that there might be an inconsistency between the data. In order to test this hypothesis, the observed precipitation and observed latent heat flux available continuously between August 16 and October 7 have been used to evaluate the moisture content with a simple water balance which is computed between two consecutive soil moisture measurements. The volumetric water content at date t_2 is calculated as

$$w(t_2) = w(t_1) + \frac{(P_{\text{obs}} - E_{\text{obs}})}{d_2 \rho_w} \tag{6}$$

where d_2 is the root depth, ρ_w is the water density, and P_{obs} and E_{obs} are the cumulative values of observed precipitation and evaporation between two dates (t_1 and t_2) of moisture measurements. The runoff rate is neglected, an assumption that sounds reasonable since the water content is far beneath the field capacity. The observed moisture content on August 16 is taken as the initial water content. The resulting moisture content (Figure 6) is much smaller than the observed one. This indicates a discrepancy between the soil moisture, the rainfall, and the evaporation measurements. According to I. R. Wright (personal communication, 1996), the soil moisture data are not completely reliable between February and October 1992.

5.2. Jaru Reserve Forest

A realistic simulation of the long-term evolution of the water content at JRF is not straightforward. During the wet season the water table rises to within 1.2 m of the soil surface and plays an important role in the water storage, but its simulation would require the use of a hydrological model. On the other hand, during the dry season the forest does not show any significant moisture stress when the water content within 3.6 m of the surface is far below the field capacity. Consequently, as mentioned before, there is strong evidence of water uptake from below a depth of 3.6 m, where no measurements are available. An effective rooting depth of 8 m, already used for the model calibration, is taken for the simulation in order to ensure enough water during the dry season. Figure 7 presents the measured volumetric water content within 3.6 m of the surface together with the simulated volumetric water content in the first 8 m of soil. The water table within 1.2 m of the surface explains why during the wet season the simulated water content is far below the observed content. During the dry season the difference between the considered depths accounts for the higher simulated water content in comparison with the observed content.

Figure 8 compares the monthly totals of the simulated evapotranspiration fluxes for the two Ji-Paraná sites (JRF, NSP). These results are averaged over the two years of simulation. The forest evaporates more than the pasture all the year round, and the evaporation does not decrease during the dry season. The interception loss also presents a marked seasonal cycle linked to the rainfall. These monthly values of interception are comparable to the values calculated by *Shuttleworth* [1988] at Reserva Ducke, a forest site near Manaus. The reduction of the interception during the dry season partly ex-

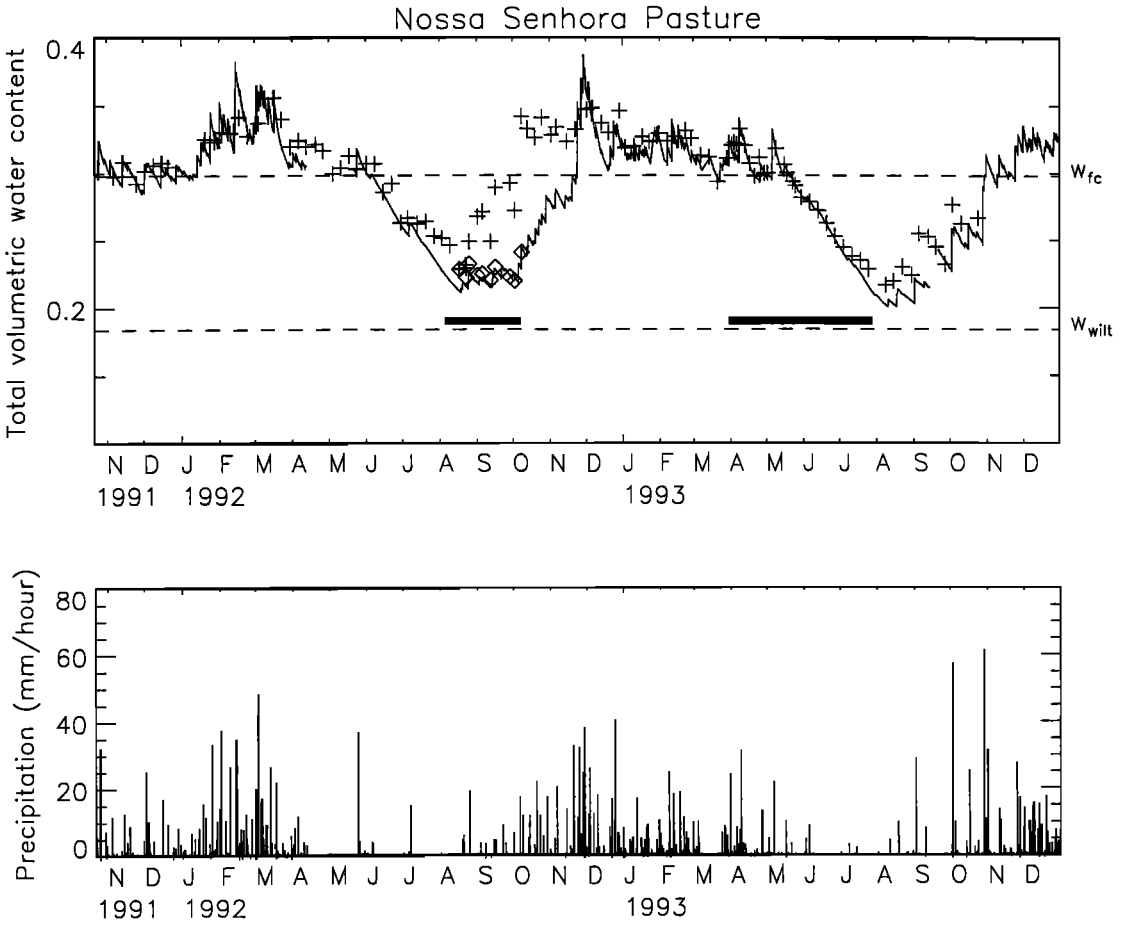

Figure 6. Evolution of the volumetric moisture content in the top 2 m simulated by ISBA-NEW over periods of continuous atmospheric forcing data (solid line) in comparison with ABRACOS moisture measurements (pluses) for the NSP site. The thick line indicates the periods of the intensive field experiments. The diamonds are the results of a hydric balance between observed precipitation and observed evaporation during an intensive field experiment. The field capacity w_{fc} and the wilting point w_{wilt} volumetric water content are indicated.

plains why the forest transpiration increases during this period. Dryer air also favors these higher transpiration rates. The smaller fraction of vegetation in the pasture explains why bare soil evaporation is higher for pasture than for forest. This evapotranspiration component also shows a seasonal cycle. The evolution of the Bowen ratio calculated with the monthly averaged fluxes (Figure 8) is very different for the two sites. The ratio for the forest remains almost constant near 0.3. In contrast, it ranges from 0.2 to 0.8 for the pasture. The decrease in evaporation during the dry season is balanced by an increase in the sensible heat flux over pastures.

5.3. Fazenda Dimona Pasture: Sensitivity to the Description of the Soil Physical Properties

The measurements taken at the FDP site were used to test the sensitivity of the simulated water budget and surface fluxes to the modified description of the soil physical properties. Two simulations were performed with the same initial conditions, clay and sand contents, and vegetation parameters: one with the original ISBA scheme (ISBA-OLD), the other with the modified version of the scheme (ISBA-NEW). The two runs differ only in the critical water contents w_{sat}, w_{fc} and w_{wilt}, the slope of the retention curve b, the saturated hydraulic conductivity, and the transfer coefficients C_2 and C_3. The values of these parameters are determined by the clay and sand contents and are calculated from the continuous relations given by *Noilhan and Lacarrère* [1995] for the "OLD" simulation and derived in section 3 for the "NEW" simulation (Table 5).

Figure 9 presents the evolution of the observed and simulated volumetric water contents over 3 years. The original version of ISBA (ISBA-OLD) clearly overestimates the water content after heavy rain. This is explained by the speed of the drainage, which is much too slow in the original ISBA scheme (ISBA-OLD). The soil at FDP has a very high clay content which is associated in the Clapp and Hornberger classification with low values of the hydraulic conductivity and, consequently, to low values of the C_3 transfer coefficient. The characteristic timescale (C_3/τ) of the drainage in the "OLD" version is of the order of 10 days whereas it is about 1 day in the "NEW" version of the scheme. This higher speed of perco-

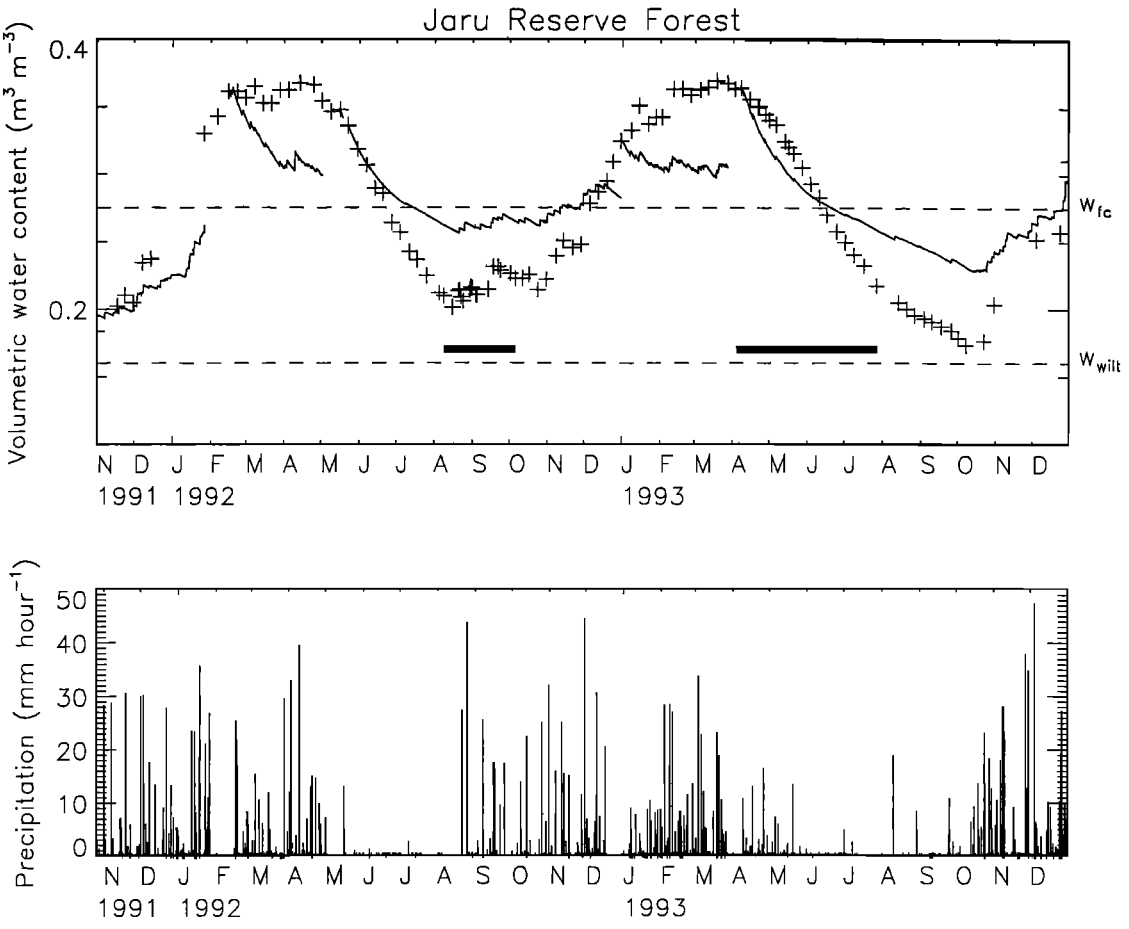

Figure 7. Evolution of the volumetric moisture content simulated by ISBA-NEW within 8 m of the surface over periods of continuous atmospheric forcing data (solid line) in comparison with ABRACOS moisture measurements taken in the first 3.6 m (pluses). The thick line indicates the periods of the intensive field experiments.

lation is in good agreement with the observations and is due to the presence of macropores at FDP, as mentioned in section 3.

In spite of the overestimation water content, the cumulated evaporation is quite similar for both runs. Transpiration differs by 11% and bare soil evaporation by 15%. This is not surprising since, more often than not, the water content is above (or near) field capacity and evapotranspiration occurs at the potential rate. Under field capacity the fact that the volumetric moisture content is set to the observed value at the beginning of each period of continuous data also plays a very important role. The real impact of the use of the Clapp and Hornberger water release model might be underestimated in this simulation due to the lack of data, which implies reinitialization of the water content. However, it seems clear that the use of this water release model highly overestimates the available water content and delays the onset of the dry season.

6. Concluding Remarks

The physical properties of some widespread Amazonian soils differ significantly from the properties of the temperate soils. The saturated hydraulic conductivity of these high-clay soils is atypically large. For these soils the deep soil percolation and the surface infiltration are much more rapid than in clayey soils of temperate regions. Saturation water content of the Amazonian soils is also larger than what is usually observed in temperate soils. Currently used land surface schemes in atmospheric modeling are based on soil water models developed for temperate regions [e.g., *Clapp and Hornberger*, 1978]. It is therefore necessary to test the validity of the parameters of these models in the case of Amazonia. Data collected during ABRACOS allowed us to reformulate the relations between texture and soil hydraulic parameters of Clapp and Hornberger's soil water model, derived by *Noilhan and Lacarrère* [1995]. These new relations were introduced in the ISBA scheme in order to simulate long-term water budget and surface energy balance of three ABRACOS sites: two pasture sites and one forest site. The thermal capacity of the vegetation and the minimum surface resistance were calibrated in order to minimize the error on the surface fluxes. This optimization was performed on periods of several weeks when flux measurements were available. The mean bias on the simulated surface fluxes over the period of calibration does not exceed 11 W m^{-2}. The long-term simulation realized with the calibrated scheme showed important differences in the evolution of the Bowen ratio in the case of forest and pasture. The Bowen ratio

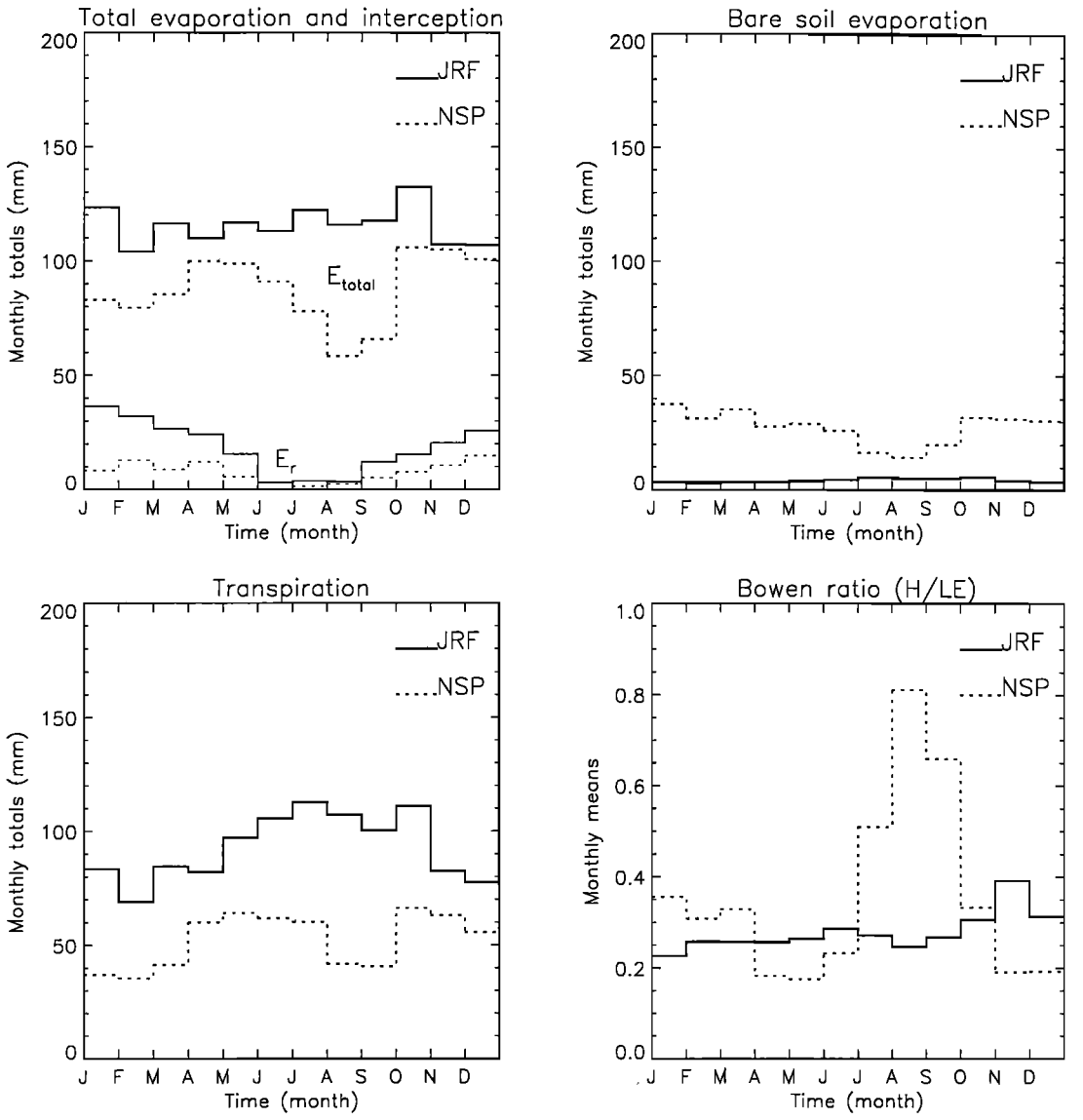

Figure 8. Annually averaged monthly totals of simulated evaporation fluxes and annually averaged monthly means of the Bowen ratio for the Jaru Reserve forest (JRF) site and the nearby Nossa Senhora pasture (NSP) site.

of the forest site remains almost constant, mainly because the hydric conditions of the soil are never limiting. The small variations in the evaporation flux are due to the interception loss directly linked to the precipitation. In the case of the pasture, the Bowen ratio increases very significantly during the dry season because of the soil moisture stress. This high value of the Bowen ratio is a direct consequence of the deforestation.

Table 5. Soil Parameters in the "NEW" and "OLD" Version of the ISBA Scheme for the Fazenda Dimona (FDP) Site

Run	w_{sat}	w_{fc}	w_{wilt}	b	C_3
NEW	0.535	0.412	0.356	20	0.962
OLD	0.481	0.405	0.324	14	0.006

The sensitivity study of the simulated soil moisture content and surface fluxes to the hydraulic properties of soils shows that the use of Clapp and Hornberger's formulation instead of the observed soil properties tends to underestimate the surface runoff. As it delays the beginning of the dry soil conditions, it also has an impact on the partitioning between surface fluxes. The use of unrealistic soil hydraulic properties may therefore have an impact on climate modeling of the Amazonian basin.

The next step of this work is the implementation of a mesoscale model including the ISBA scheme in the Amazonian area. Recently, *Calvet et al.* [1996] have processed vegetation and soil maps of a 500 km × 500 km domain centered on the Ji-Paraná sites. This information will be combined with the calibration of ISBA and the hydraulic properties of the Amazonian soils described here in order to simulate the impact of deforestation on the mesoscale meteorology.

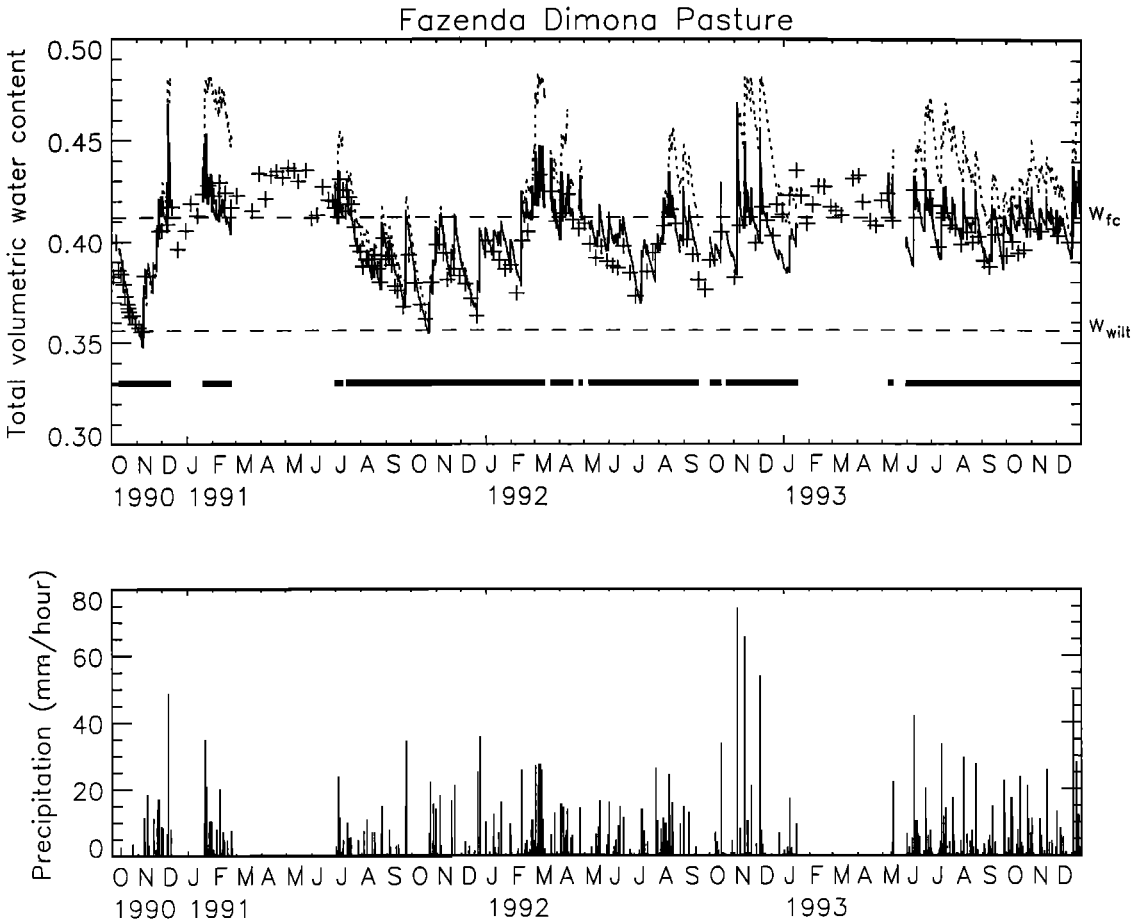

Figure 9. Evolution of the volumetric moisture content within 1.5 m of the surface simulated by ISBA-OLD (dotted line) and ISBA-NEW (solid line) over periods of continuous atmospheric forcing data in comparison with ABRACOS moisture measurements (pluses). The thick line indicates the periods of continuous atmospheric forcing data.

Appendix: Brief Description of ISBA

The ISBA scheme computes mainly the evolution of five prognostic variables: the deep soil temperature T_2, the deep soil water content w_2, a common temperature for soil surface and vegetation T_s, the topsoil water content w_g, and the interception water storage W_r. The five prognostic equations are

$$\frac{\partial T_s}{\partial t} = C_T(R_n - H - LE) - \frac{2\pi}{\tau}(T_s - T_2) \quad \text{(A1)}$$

$$\frac{\partial T_2}{\partial t} = \frac{1}{\tau}(T_s - T_2) \quad \text{(A2)}$$

$$\frac{\partial w_g}{\partial t} = \frac{C_1}{\rho_w d_1}(P_g - E_g) - \frac{C_2}{\tau}(w_g - w_{geq}) \quad \text{(A3)}$$

$$0 \le w_g \le w_{sat}$$

$$\frac{\partial w_2}{\partial t} = \frac{1}{\rho_w d_2}(P_g - E_g - E_{tr}) - \frac{C_3}{d_2\tau}\max[0, (w_2 - w_{fc})] \quad \text{(A4)}$$

$$0 \le w_2 \le w_{sat}$$

$$\frac{\partial W_r}{\partial t} = \text{veg}P - E_r - R_r \qquad 0 \le W_r \le W_{rmax} \quad \text{(A5)}$$

where veg is the fractional vegetation cover. The hydric and thermal transfer coefficients are given as

$$C_T = \left[\frac{\text{veg}}{C_n} + \frac{1 - \text{veg}}{C_g}\right]^{-1} \quad \text{(A6)}$$

$$C_g = C_{gsat}\left(\frac{w_{sat}}{w_2}\right)^{b/(2\ln 10)} \quad \text{(A7)}$$

$$C_1 = C_{1sat}\left(\frac{w_{sat}}{w_g}\right)^{1+(b/2)} \quad \text{(A8)}$$

$$C_2 = C_{2ref}\left(\frac{w_2}{w_{sat} - w_2 + \varepsilon}\right) \quad \text{(A9)}$$

$$C_3 = \frac{\tau(2b + 2)K_{sat}}{w_{sat}[(w_{sat}/\tilde{w}_2)^{2b+2} - 1]} \quad \text{(A10)}$$

where ε is a small numerical value which limits C_2 at saturation and $\tilde{w}_2$ is defined as

$$\ln\left(\frac{w_{sat} - w_{fc}}{\tilde{w}_2 - w_{fc}}\right) = 1 \quad \text{(A11)}$$

A list of symbols is given in the notation section. The scheme also includes a representation of snow, which is not described

here [*Douville et al.*, 1995]. An updated description of the scheme is presented by *Noilhan and Mahfouf* [1996], as well as a summary of the various calibration studies already performed.

The turbulent fluxes are calculated by means of the classical aerodynamic formulae [*Louis*, 1979]. For the sensible heat flux

$$H = \rho_a C_p (T_s - T_a)/R_a \tag{A12}$$

where R_a, the aerodynamic resistance, is given as

$$R_a = (C_H V_a)^{-1} \tag{A13}$$

and where C_p is the specific heat of air; ρ_a, V_a, and T_a are respectively the air density, the wind speed, and the temperature at the lowest atmospheric level; and C_H is the drag coefficient depending upon the thermal stability of the atmosphere. The water vapor flux E is the sum of the evaporation from the soil surface E_g, the transpiration of the vegetation E_{tr}, and the evaporation of the water intercepted by the canopy E_r:

$$E_g = (1 - \text{veg})\rho_a \frac{(h_u q_{\text{sat}}(T_s) - q_a)}{R_a} \tag{A14}$$

$$E_{tr} = \text{veg} \frac{1 - \delta}{R_a + R_s} (q_{\text{sat}}(T_s) - q_a) \tag{A15}$$

$$E_r = \text{veg} \frac{\delta}{R_a} (q_{\text{sat}}(T_s) - q_a) \tag{A16}$$

where $q_{\text{sat}}(T_s)$ is the saturated specific humidity at the temperature T_s, q_a is the atmospheric specific humidity at the lowest atmospheric level, and h_u is the relative humidity at the ground surface. Here δ is the fraction of the foliage covered by intercepted water. For the pasture, δ is approximated by a power function of the moisture content of the interception reservoir [*Deardorff*, 1978]:

$$\delta = (W_r/W_{r\max})^{2/3} \tag{A17}$$

For the forest the wet fraction of the canopy is calculated using the parameterization for tropical forest proposed by *Manzi* [1993]:

$$\delta = \frac{W_r}{((1 + \frac{7}{3}\text{LAI})W_{r\max} - \frac{7}{3}W_r)} \tag{A18}$$

The canopy surface resistance, R_s is calculated as

$$R_s = \frac{R_{s\min}}{\text{LAI}} F_1 F_2 F_3 F_4 \tag{A19}$$

where the functions F_1, F_2, F_3, and F_4 depend upon radiation, air temperature and humidity, and available water in the soil.

Notation

T_s surface temperature.
T_2 deep soil temperature.
w_g topsoil volumetric water content.
w_2 deep soil volumetric water content.
W_R intercepted water by the canopy.
P, P_g precipitation at screen and ground level.
R_n net radiation.
R_G incoming solar radiation.
G soil heat flux.
H sensible heat flux.
E total evapotranspiration.
E_v evapotranspiration from the vegetation.
E_{tr} transpiration.
E_g surface evaporation from bare soil.
E_r evaporation from intercepted water.
R_r runoff from interception water reservoir.
C_1, C_2 force restore coefficients for soil moisture.
C_3 coefficient for gravitational drainage.
C_T surface soil/vegetation thermal transfer coefficient.
C_g surface bare soil thermal transfer coefficient.
C_v vegetation thermal transfer coefficient.
ρ_w density of liquid water.
d_1, d_2 depths of the topsoil and deep soil.
τ time constant of 1 day.
w_{sat} saturated volumetric moisture content.
w_{fc} field capacity volumetric moisture content.
w_{wilt} wilting point volumetric moisture content.
b slope of the retention curve.
$C_{G\text{sat}}$ soil thermal coefficient at saturation.
$C_{1\text{sat}}$ value of C_1 at saturation.
$C_{2\text{ref}}$ value of C_2 at $w_2 = 0.5w_{\text{sat}}$.
a, p coefficients of w_{geq} formulation.
d_2 depth of soil column.
$R_{s\min}$ minimum leaf stomatal resistance.
LAI leaf area index.
veg vegetation cover.
z_0 roughness length.
α_t surface albedo.
ε_t emissivity.

References

Alvalá, R. S., R. Gielow, I. Wright, and M. Hodnett, Thermal diffusivity of Amazonian soils, in *Amazonian Deforestation and Climate*, edited by J. H. Gash, C. A. Nobre, J. Roberts, and R. L. Victoria, pp. 139–150, John Wiley, New York, 1996.

Bhumralkar, C. M., Numerical experiments on the computation of ground surface temperature in an atmospheric circulation model, *J. Appl. Meteorol.*, *14*, 1246–1258, 1975.

Calvet, J.-C., R. Santos-Alvalá, G. Jaubert, C. Delire, C. Nobre, I. Wright, and J. Noilhan, Mapping surface parameters for mesoscale modeling in forested and deforested south-western Amazonia, *Bull. Am. Meteorol. Soc.*, *78*(3), 413–423, 1997.

Clapp, R. B., and G. M. Hornberger, Empirical equations for some hydraulic properties, *Water Resour. Res.*, *14*, 601–604, 1978.

Cuenca, R. H., M. Ek, and L. Mahrt, Impact of soil water property parameterization on atmospheric boundary layer simulation, *J. Geophys. Res.*, *101*, 7269–7277, 1996.

Culf, A. D., G. Fish, and M. Hodnett, The albedo of Amazonian forest and ranch land, *J. Clim.*, *8*, 1544–1554, 1995.

da Rocha, H., P. Sellers, G. Collatz, I. Wright, and J. Grace, Calibration and use of the SiB2 model to estimate water vapour and carbon exchange at the ABRACOS forest sites, in *Amazonian Deforestation and Climate*, edited by J. H. C. Gash et al., pp. 459–471, John Wiley, New York, 1996a.

da Rocha, H., C. Nobre, J. Bonatti, I. Wright, and P. Sellers, A vegetation-atmosphere interaction study for Amazonia deforestation using field data and a "single column" model, *Q. J. R. Meteorol. Soc.*, *122*, 567–594, 1996b.

Deardorff, J. W., Efficient prediction of ground surface temperature and moisture with inclusion of a layer of vegetation, *J. Geophys. Res.*, *83*, 1889–1903, 1978.

Dickinson, R. E., and A. Henderson-Sellers, Modelling tropical deforestation: A study of GCM land-surface parameterizations, *Q. J. R. Meteorol. Soc.*, *114*, 439–462, 1988.

Douville, H., J.-F. Royer, and J.-F. Mahfouf, A new snow parameterization for the Météo-France climate model, *Clim. Dyn.*, *12*, 21–52, 1995.

Eltahir, E., and R. Bras, On the response of the tropical atmosphere to large-scale deforestation, *Q. J. R. Meteorol. Soc.*, *119*, 779–793, 1993.

Gash, J., C. Nobre, J. Roberts, and R. Victoria, An overview of ABRACOS, in *Amazonian Deforestation and Climate*, edited by J. Gash et al., pp. 1–14, John Wiley, New York, 1996.

Hodnett, M., L. da Silva, H. da Rocha, and R. C. Senna, Seasonal water storage changes beneath central Amazonian rainforest and pasture, *J. Hydrol.*, *170*, 233–254, 1995.

Hodnett, M., M. Oyama, J. Tomasella, and A. de O. Marques Filho, Comparison of long-term soil water storage behaviour under pasture and forest in three areas of Amazonia, in *Amazonian Deforestation and Climate*, edited by J. H. Gash, C. A. Nobre, J. Roberts, and R. L. Victoria, pp. 57–77, John Wiley, New York, 1996a.

Hodnett, M., J. Tomasella, A. de O. Marques Filho, and M. Oyama, Deep soil water uptake by forest and pasture in central Amazonia: Predictions from long-term daily rainfall data using a simple water balance model, in *Amazonian Deforestation and Climate*, edited by J. H. Gash et al., pp. 79–99, John Wiley, New York, 1996b.

Jacquemin, B., and J. Noilhan, Sensitivity study and validation of a land surface parameterization using the HAPEX-MOBILHY dataset, *Boundary Layer Meteorol.*, *52*, 93–134, 1990.

Kern, J. S., Evaluation of soil water retention models based on basic soil physical properties, *Soil Sci. Soc. Am. J.*, *59*, 1134–1141, 1995.

Lean, J., and D. Warrilow, Simulation of the regional climatic impact of Amazon deforestation, *Nature*, *342*, 411–413, 1989.

Louis, J., A parametric model of vertical eddy fluxes in the atmosphere, *Boundary Layer Meteorol.*, *17*, 187–202, 1979.

Mahfouf, J.-F., and J. Noilhan, Comparative study of various formulations of evaporation from bare soil using in situ data, *J. Appl. Meteorol.*, *30*(9), 1354–1365, 1991.

Mahfouf, J.-F., and J. Noilhan, Inclusion of gravitational drainage in a land surface scheme based on the force restore method, *J. Appl. Meteorol.*, *35*(6), 987–992, 1996.

Manzi, A., Introduction d'un schéma des transferts sol-végétation-atmosphère dans un modèle de circulation générale et application à la simulation de la déforestation amazonienne, Ph.D. thesis, Univ. Paul Sabatier, Toulouse, France, 1993.

Manzi, A., and S. Planton, Calibration of a GCM using ABRACOS and ARME data and simulation of Amazonian deforestation, in *Amazonian Deforestation and Climate*, edited by J. H. C. Gash et al., pp. 505–529, John Wiley, New York, 1996.

McCumber, M. C., and R. A. Pielke, Simulation of the effects of surface fluxes of heat and moisture in a mesoscale numerical model, *J. Geophys. Res.*, *86*, 9929–9938, 1981.

McWilliam, A.-L., O. Cabral, B. Gomes, J. Esteves, and J. Roberts, Forest and pasture leaf-gas exchange in south-west Amazonia, in *Amazonian Deforestation and Climate*, edited by J. H. C. Gash et al., pp. 265–285, John Wiley, New York, 1996.

Moore, C., and G. Fisch, Estimating heat storage in Amazonian tropical forest, *Agric. For. Meteorol.*, *38*, 147–169, 1986.

Mualem, Y., A new model for predicting the hydraulic conductivity of unsaturated porous media, *Water Resour. Res.*, *12*, 513–522, 1976.

Nobre, C., P. Sellers, and J. Shukla, Amazonian deforestation and regional climate change, *J. Clim.*, *4*, 957–988, 1991.

Noilhan, J., and P. Lacarrère, GCM grid-scale evaporation from mesoscale modeling, *J. Clim.*, *8*(2), 206–223, 1995.

Noilhan, J., and J.-F. Mahfouf, The ISBA land surface parameterisation scheme, *Global Planet. Change*, *13*, 145–159, 1996.

Noilhan, J., and S. Planton, A simple parameterization of land surface processes for meteorological models, *Mon. Weather Rev.*, *117*, 536–549, 1989.

Polcher, J., and K. Laval, The impact of African and Amazonian deforestation on tropical climate, *J. Hydrol.*, *155*, 389–405, 1994.

RADAMBRASIL Projeto, Levantamento dos recursos naturais, *Tech. Rep. 16:SC-20*, Porto Velho, Brazil, 1978. (Available from IBGE/CDDI, Marcanã, Rio de Janeiro, Brazil.)

Roberts, J., O. Cabral, J. da Costa, A.-L. McWilliam, and T. de A. Sà, An overview of the leaf area index and physiological measurements during ABRACOS, in *Amazonian Deforestation and Climate*, edited by J. H. C. Gash et al., pp. 459–471, John Wiley, New York, 1996.

Sellers, P. J., Y. C. Sud, and A. Dalcher, A simple biosphere model (SiB) for use within general circulation models, *J. Atmos. Sci.*, *43*, 505–531, 1986.

Shuttleworth, J. W., Evaporation from Amazonian rainforest, *Proc. R. Soc. London, Ser. B*, *233*, 321–346, 1988.

Shuttleworth, J. W., et al., Eddy correlation measurements of energy partition for Amazonian forest, *Q. J. R. Meteorol. Soc.*, *110*, 1143–1162, 1984.

Staley, D. O., and G. M. Jurica, Effective atmospheric emissivity under clear skies, *J. Appl. Meteorol.*, *11*, 349–356, 1972.

Stieglitz, M., D. Rind, J. Famiglietti, and C. Rosenzweig, An efficient approach to modeling the topographic control of surface hydrology for regional and global climate modeling, *J. Clim.*, *10*, 118–137, 1997.

Tomasella, J., and M. G. Hodnett, Soil hydraulic properties and van Genuchten parameters for an Oxisol under pasture in central Amazonia, in *Amazonian Deforestation and Climate*, edited by J. H. C. Gash et al., pp. 101–124, John Wiley, New York, 1996.

van Genuchten, M. T., A closed formulation for predicting hydraulic conductivity in unsaturated soils, *Soil Sci. Soc. Am. J.*, *44*, 892–898, 1980.

Wright, I., J. Gash, H. da Rocha, W. Shuttleworth, C. Nobre, G. Maitelli, C. Zamparoni, and P. Carvalho, Dry season micrometeorology of central Amazonian ranchland, *Q. J. R. Meteorol. Soc.*, *118*, 1083–1099, 1992.

Wright, I. R., C. A. Nobre, J. Tomasella, H. R. da Rocha, J. M. Roberts, E. Vertamatti, A. D. Culf, R. C. S. Alvalà, M. G. Hodnett, and V. N. Ubarana, Towards a GCM surface parameterization of Amazonia, in *Amazonian Deforestation and Climate*, edited by J. H. C. Gash et al., pp. 474–504, John Wiley, New York, 1996.

Xue, Y., H. Bastable, P. Dirmeyer, and P. Sellers, Sensitivity of simulated surface fluxes to changes in land surface parameterizations—A study using ABRACOS data, *J. Appl. Meteorol.*, *35*, 386–400, 1996.

Zhang, H., A. Henderson-Sellers, and K. M. Guffie, Impacts of tropical deforestation, 1, Processes of local climatic change, *J. Clim.*, *9*, 1497–1517, 1996.

J.-C. Calvet, C. Delire, and J. Noilhan, Météo-France/Centre National de la Recherche Météorologique, 42, avenue Gaspard Coriolis, 31057 Toulouse Cedex, France. (e-mail: delire@cnrm.meteo.fr)

A. Manzi and C. Nobre, Centro de Previsão de Tempo Estudios Climaticos, Instituto Nacional de Pesquisas Espaciais, Rodovia Presidente Dutra, km 40, C.P. 01, 12.630-000 Cachoeira Paulista, São Paulo, Brazil.

I. Wright, Institute of Hydrology, Maclean Building, Crowmarsh Gifford, Wallingford, Oxfordshire OX10 8BB, England, United Kingdom.

(Received December 11, 1996; revised June 18, 1997;
accepted June 18, 1997.)